

Crystallization properties of ^3He - ^4He solutions at low temperatures

V. N. Lopatik

Institute of Physics Problems, Academy of Sciences of the USSR, Moscow

(Submitted 2 June 1983)

Zh. Eksp. Teor. Fiz. **86**, 487-496 (February 1984)

The crystallization curves of 0-20% ^3He solutions in ^4He have been measured at temperatures between 0.03 and 1.2 K. As well as the minima, maxima were found on these curves at $T = 0.28$ K. The dependence of the limiting crystallization pressure at $T = 0$ on concentration due to the osmotic pressure of ^3He in the liquid phase, was determined. The melting curves of weak mixtures were deduced from the crystallization curves. The emergence of the crystallization curves onto the triple line is discussed. $T - x$ diagrams of state for $p = \text{const}$ are plotted.

Much work has been devoted to investigating the phase diagrams and properties of ^3He - ^4He solutions (see review of Ref. 1) However, the region of small ^3He concentrations and low temperatures remains insufficiently studied. The necessity of investigating the diagrams of state for weak solutions arose in connection with increasing interest in the properties of dilute ^3He - ^4He solutions at ultralow temperatures. We have extended the study of weak solutions² down to concentrations at which stratification starts.

In the present work we have studied the temperature dependence of the start of crystallization of ^3He - ^4He mixtures in the range 0.03-1.2 K for solutions containing up to 20% ^3He . Measurements were made of the crystallization curves for non-separated solutions and also of the triple line when liquid separated into two phases is crystallizing.

Work in this region is complicated by the existence of minima in the melting and crystallization curves, so that the measurements were carried out in a Pomeranchuk cell. A description of the apparatus, consisting of two separated volumes which could be varied with the help of two connected bellows, was given before.²

A ^3He - ^4He mixture of given concentration was condensed into the working volume ($V \approx 12 \text{ cm}^3$) through a fine capillary tube, and a pressure just below the minimum crystallization pressure was generated in it by a gasifier, after which the mixture was shut off from external connections by a valve. The volume of the capillaries ($V \approx 0.05 \text{ cm}^3$) was small compared with the cell volume. The mixture was made up in a separate bulb and was condensed in small portions, so that the concentration of the mixture remaining in the bulb was always constant. There was a carbon thermometer in the cell, calibrated by the susceptibility of cerium magnesium nitrate, and the temperature was measured by this.

Heat exchange in the cell was achieved through a copper heat exchanger consisting of a 20 cm^2 area copper plate, both sides of which had copper powder pressed in to a depth of 0.5 mm, the grain size being about $10 \mu\text{m}$ and filling factor 0.5. The effective heat exchange surface $S_{\text{eff}} \approx 0.2 \text{ m}^2$. The heat-exchanger was placed between the bellows and the cell wall over the whole perimeter and was connected through a thermal switch to a dilution cryostat. The mixture was cooled with the help of the dilution cryostat, by which a temperature down to 25 mK could be obtained inside the Pomeranchuk cell. The pressure was measured by a capaci-

tance gauge to high accuracy (10^{-3} atm). The 0.5 mm thick cell walls (the cell was made of bronze) acted as one of the capacitor plates. A coaxial bronze conical cylinder served as the second plate, laid along the body and insulated from it by linings. The pressure-dependent capacitance together with an inductance formed the resonant circuit of an oscillator. The sensitivity of the gauge was 5 kHz/atm.

The measurements were made in the following way. A mixture of fixed concentration was condensed at $T \approx 1.2 \text{ K}$ in the mixture cell and shut off at a certain pressure, while pure ^4He from a high pressure cylinder was condensed in the other chamber. The mixture was then cooled with the dilution cryostat, and by raising the pressure in the ^4He chamber the mixture in the measuring cell was compressed at a fixed temperature. The pressure change in the mixture was continuously recorded on a chart recorder. The pressure in the measuring cell grew together with the ^4He pressure while there was only liquid in it. The start of crystallization was marked by an abrupt halt to the pressure increase in the mixture while the ^4He supply continued.

The concentration of the crystal formed is in general different from the liquid phase concentration. For this reason the concentration of the liquid phase changes as the crystal grows and to obtain a definite result it is essential to fix the moment at which only an insignificant amount of solid phase is formed, i.e., to fix the actual start of crystallization.

We grew about 0.2 cm^3 of crystal, an amount which did not affect the concentration, was much more than the volume of the capillaries, and showed that the growing crystal was in the chamber and not in the connections.

The process of crystal formation and growth did not proceed identically over the whole temperature range and depended on the region of the phase diagram where crystallization was taking place. At temperatures above 0.4 K and below 0.1 K there was no difficulty in forming and melting a crystal. For sufficiently slow raising of the ^4He pressure, the increase in the pressure in the mixture abruptly ended at the start of crystallization and crystal formation proceeded at constant pressure. For crystal formation to start in the region of the maxima in the range $0.1 < T < 0.4 \text{ K}$, it was essential to provide a liquid-mixture pressure in excess of the equilibrium crystallization pressure. The pressure in the mixture fell after the start of crystallization as the crystal grew, up to some value, and crystal growth proceeded further at this

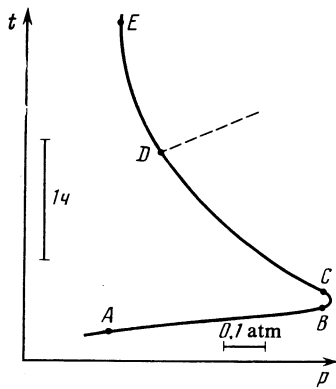


FIG. 1. Plot of the pressure in the cell on crystallization of a stratified mixture near the maximum; *AB*—compression of the liquid phase; *B*—start of crystallization; *C*—cessation of ^4He supply to the auxiliary cell; *CDE*—slow crystal growth, the return of the pressure to the equilibrium value; *E*—equilibrium crystallization pressure; dashed line—plot of pressure on repeating the ^4He supply to the auxiliary cell.

constant pressure although the supply of ^4He continued. The value of the excess pressure depended on temperature and concentration and increased on approaching the maximum with increasing concentration, reaching about 0.05 atm. Starting with a concentration of about 11% at $T = 0.28$ K, the nature of the crystallization in the region of the maximum changed sharply. It was necessary to provide an excess pressure more than 0.5 atm to start crystal formation and further crystal growth proceeded very slowly.

If the ^4He supply was resumed, the pressure in the mixture grew in spite of the growth of the crystal. For constant ^4He pressure the crystal grew for about 2 h before the pressure took up its equilibrium value for the liquid-crystal system at the given temperature (Fig. 1). Such a crystallization characteristic covered the temperature interval from 0.28 to 0.21 K for the 11% mixture. The formation of a crystal in the same way for larger concentrations on the triple line occurred in the region of its maximum for a temperature between 0.2 and 0.36 K. It is possible that this is connected with the occurrence of stratification in the solutions and

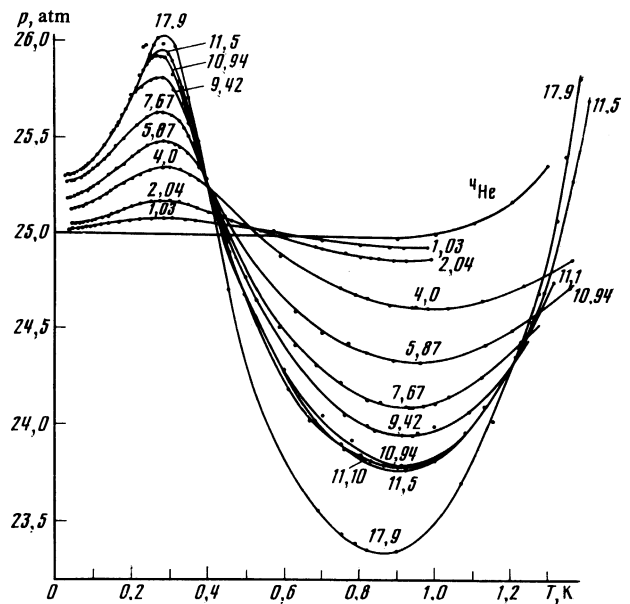


FIG. 2. Curves of the start of crystallization of ^3He - ^4He mixtures. The numbers indicate the ^3He content in %.

with the complicated structure of the phase diagram in this region.³ In addition, a very slow (about two hours) establishment of concentration equilibrium was found by Fenner and Luszczynski⁴ in a stratified liquid in a cell of dimensions 2 cm.

Solidification curves for eleven different solution concentrations, including pure ^4He , are shown in Fig. 2. (The values of the crystallization pressures are given in Table I.) The reconciliation and calibration were against pure ^4He (Ref. 5). Apart from the already known minima, there are maxima on the curves for all concentrations at about one and the same temperature $T_{\text{max}} = 0.28$ K. The crystallization pressure at the maximum increases proportionately with concentration, reaching a maximum value ≈ 26 atm at the

TABLE I. Crystallization curves for ^3He - ^4He mixtures.

T, K	x, % He ³							
	1.03	2.04	4.0	5.87	7.67	9.42	11.5	17.9
0.05	25.02	25.05	25.13	25.19	25.22	25.31	25.31	25.31
0.1	25.03	25.07	25.17	25.24	25.33	25.38	25.38	25.38
0.15	25.05	25.10	25.22	25.31	25.43	25.52	25.52	25.52
0.2	25.07	25.14	25.28	25.40	25.54	25.71	25.71	25.71
0.25	25.08	25.17	25.33	25.47	25.62	25.80	25.92	25.95
0.28	25.08	25.17	25.34	25.48	25.63	25.82	25.95	26.03
0.3	25.08	25.17	25.34	25.48	25.62	25.79	25.91	26.02
0.35	25.07	25.15	25.31	25.44	25.50	25.55	25.61	25.68
0.4	25.06	25.12	25.23	25.27	25.25	25.23	25.21	25.20
0.45	25.04	25.08	25.14	25.06	25.01	24.98	24.90	24.75
0.5	25.03	25.04	25.05	24.90	24.81	24.76	24.66	24.33
0.6	25.01	24.98	24.88	24.67	24.50	24.42	24.28	23.82
0.7	24.97	24.93	24.77	24.50	24.30	24.19	24.00	23.55
0.8	24.96	24.90	24.68	24.40	24.17	24.03	23.85	23.38
0.9	24.94	24.87	24.64	24.35	24.11	23.97	23.78	23.36
1.0	24.95	24.89	24.63	24.35	24.13	24.00	23.84	23.50
1.1	—	—	24.65	24.41	24.23	24.10	24.02	23.85
1.2	—	—	24.72	24.52	24.40	24.34	24.32	24.30

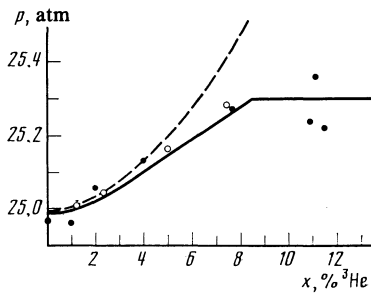


FIG. 3. Limiting crystallization pressures of weak solutions for $T = 0$: (●) results of the present work, (○) results calculated according to the osmotic pressure,⁹ dashed line—kinetic contribution, full line theoretical curves according to Ebner and Edwards.¹²

triple line. A parabolic form of curves ($\Delta p \propto T^2$) is observed for $T \rightarrow 0$. This is explained qualitatively by the fact that the solubility of ^3He in the solid phase is vanishingly small at the lowest temperatures and the slope of the curves is determined by the entropy of the liquid phase, which gives $dp/dT \propto T$ and $\Delta p \propto T^2$. The solubility of ^3He in the solid phase increases with increasing temperature, the entropy of the solid becomes greater than that of the liquid and the crystallization curve takes on a negative, Pomeranchuk, slope passing through a maximum. The parabolic behavior of the curves shows that for $T \rightarrow 0$ a solid phase with vanishingly small ^3He concentration is formed. This agrees with the fact that as $T \rightarrow 0$ solid solutions separate into practically pure components, i.e., solid solutions do not exist at 0 K.

The crystallization pressure at $T = 0$ is not equal to 25 atm, as for pure ^4He , but depends on the concentration of the mixture from which the crystals are formed. The dependence of the limiting pressure on mixture concentration at $T = 0$ is shown in Fig. 3. The pressure increases from 25 atm for pure ^4He to 25.3 atm for a mixture containing about 8.5% ^3He . This is the limiting concentration for which stratification of the solution for the given pressure takes place for $T = 0$.⁶ The crystallization pressure for $T = 0$ remains constant further along the triple line in a stratified solution. The increase in the limiting pressure with increasing concentration of the solution⁷ is explained by the fact that in equilibrium the partial chemical potentials of ^4He in the solid phase and in the solution must be equal:

$$v_S \Delta p(x) = v_L \Delta p(x) - \pi(x) v_L,$$

where v_S and v_L are the volumes per particle in the solid and liquid phases. This condition leads to the following expression for the crystallization pressure for $T = 0$:

$$p^* = p_0 + \Delta p(x) = p_0 + \pi(x) v_L / (v_L - v_S),$$

where $\pi(x)$ corresponds to the osmotic pressure of a degenerate Fermi gas of concentration x .

Using data on the heat of mixing, Seligmann *et al.*⁸ were able to calculate the osmotic pressure at zero temperature. The results obtained by Landau *et al.*^{6,9} in experiments to measure the osmotic pressure of ^3He in dilute solutions agree well with these calculations. The open circles in Fig. 3 show the values of crystallization pressure for various concentra-

tions at $T = 0$, calculated on the basis of the results obtained by Landau *et al.* for the osmotic pressure at a mixture pressure of 20 atm, which agrees well with the results obtained by us.

The interaction of ^3He atoms with one another has to be taken into account for the concentrations considered in this work when calculating the osmotic pressure. Apart from the "ideal" kinetic part

$$\pi_k(x) = \frac{2}{3} \bar{E} = \frac{2}{5} \frac{p_F^2}{2m^*} n_4 x,$$

where m^* is the effective mass of ^3He atoms, n_4 is the number density of ^4He atoms, $p_F = \hbar(3\pi^2 n_4)^{1/3} x^{1/3}$ is the Fermi momentum for a solution of concentration x , there is another contribution to the osmotic pressure produced by the potential energy due to the weak nonideality of the degenerate Fermi gas of impurity quasiparticles.

The kinetic contribution to the change in limiting crystallization pressure $\Delta p_k \propto x^{5/3}$, is shown by the dashed line in Fig. 3. The potential contribution to the osmotic pressure, $-\pi_p(x)$, is calculated by using the effective interaction potential between the impurity particles. From data on spin diffusion of ^3He in solution, which gives the form of the effective potential, Bardeen *et al.*¹⁰ determined its parameters and then by using this potential they calculated other properties of degenerate solutions. Baym and Ebner¹¹ (see also the review 12), using more experimental data, also chose an effective potential which describes well the properties of degenerate solutions. The partial impurity pressure (the contribution to the crystallization pressure at $T = 0$) for vanishingly small concentrations ($x \leq 1\%$) is given by Bashkin and Meierovich.¹ Values of the osmotic pressure $\pi(x) = \pi_k(x) - \pi_p(x)$, calculated on taking account of the interaction of impurity ^3He quasiparticles, give good agreement with our experimental results.

Measurements of the triple line in the region of the maximum and at lower temperatures are shown in Fig. 2.

On lowering the temperature, liquid ^3He - ^4He mixtures separate into two immiscible liquids with different ^3He concentrations. The stratification temperature depends on the concentration of the mixture and on pressure. The stratification curves for different pressures were measured by Zinov'eva.¹³ However, there exists a limiting ^3He concentration, below which the mixture does not stratify even at $T = 0$ K. The pressure dependence of the limiting ^3He concentration for $T = 0$ K has been measured by Landau *et al.*⁶ and by Watson *et al.*¹⁴

On crystallization of a stratified mixture, three phases exist simultaneously and their concentrations are independent of the initial concentration of the mixture but depend only on temperature. The crystallization curves of stratified solutions therefore coincide with and form the triple line. As can be seen from the graphs of Fig. 2, the crystallization curves of mixtures go over to the triple line at the temperature where the mixture of the given concentration stratifies. As the concentration is reduced, stratification and going over to the triple line occur at a lower temperature, and correspondingly the sections where the crystallization curves coincide decrease. For mixtures with ^3He concentrations

7.67% and less, the forms of crystallization curves differ from one another even for the lowest temperature and do not coincide on extrapolation of the ends to $T = 0$. It follows from this that passage to the triple line for $T = 0$ and $p \approx 25$ atm occurs with mixtures having ^3He concentration more than 8%, which agrees with the results of Landau *et al.*⁶ and of Watson *et al.*,¹⁴ but disagrees with those obtained by van den Brandt *et al.*¹⁵

At $T = 0$ the triple line has a pressure of 25.3 atm, which increases with increasing temperature and reaches a maximum pressure of 26 atm at $T = 0.28$ K.

According to earlier work,^{3,16} there is a quadruple point at the vertex of the triple line, where four triple lines meet, and at a temperature below $T_{\text{max}} = 0.28$ K the solution crystallizes in the hexagonal close packed (hcp) phase, while above 0.28 it crystallizes in the body centered cubic (bcc) phase. As is known,¹⁷ pure ^4He crystallizes in the bcc phase in the temperature interval 1.45–1.77 K, while below 1.45 K it crystallizes in the hcp phase. The bcc phase rapidly expands with increasing concentration of the mixture.^{18,19} By taking this into account and starting from the present measurements of the crystallization curves, the approximate behavior of the hcp-bcc-liquid triple line in the p - T plane can be plotted (Fig. 4). This triple line goes to the quadruple point Q_1 under the bcc- L_1 - L_2 triple line, unlike what was considered earlier^{3,16} (L_1 is the ^4He saturated liquid phase, L_2 is the ^3He saturated liquid phase). This fact is considered in more detail when plotting the T - x phase diagram for $p = \text{const}$.

On crystallization of a solution, the ^3He concentration in the solid phase differs from the concentration in the liquid and it changes continuously as the crystal grows. This makes the preparation of uniform solid mixtures and the direct determination of melting curves extremely difficult. However, melting curves can be established from crystallization curves. This can be done with the help of the Clausius-Clapeyron equation for the melting curve

$$\frac{dp_{\text{melt}}}{dT} = \frac{x_L(s_3^L - s_3^S) + (1 - x_L)(s_4^L - s_4^S)}{x_L(v_3^L - v_3^S) + (1 - x_L)(v_4^L - v_4^S)}$$

In the temperature region where the interaction of impurity atoms with each other can be neglected, a simpler equation

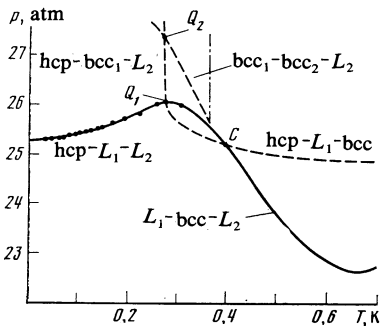


FIG. 4. Projections of three-phase lines near the quadruple point Q_1 onto the p - T plane. Points—results of the present work, full line—results of Vvedenskii.³ bcc_1 , bcc_2 are the bcc phases corresponding to smaller and larger ^3He concentrations; dashed-dot—line of critical points of the bcc_1 - bcc_2 stratification surface.

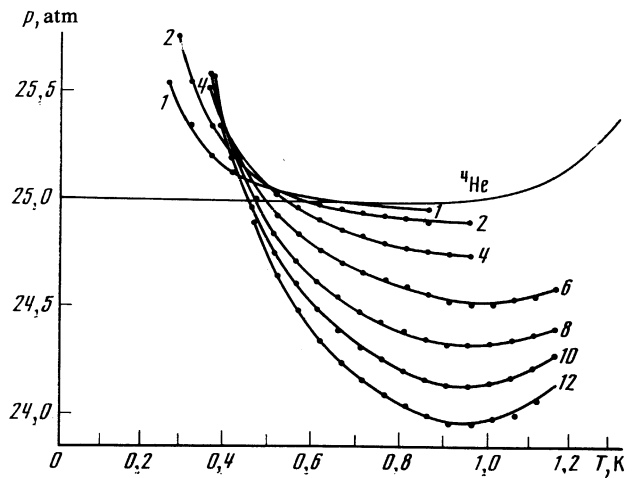


FIG. 5. Melting curves constructed from the crystallization curves. The numbers indicate the ^3He content in %.

can be used to establish the melting curve. This is possible for $T > T_F$ for liquid mixtures (T_F is the Fermi temperature for a mixture of the given concentration); the interaction can be neglected over the whole temperature range studied for solid mixtures. We then have²⁰ for the shift in the crystallization curve relative to that for pure ^4He

$$\Delta p = T(x_L - x_S) / (v_4^L - v_4^S)$$

The concentration x_S of the solid phase in an equilibrium with the liquid phase of a given concentration can easily be determined from this. Melting curves established in this way are shown in Fig. 5. It can be seen that there are minima in the melting curves, and as the temperature is lowered the pressure at which solid mixtures start to melt increases sharply. This agrees with the fact that at temperatures below about 0.2 K solid solutions in the equilibrium state separate into almost the pure components.²¹

It follows from the above equation that at the points of intersection of the crystallization curves of the mixture with the curve for pure ^4He , $\Delta p = 0$ and consequently the concentrations in the solid and liquid phases are the same. The crossing points thus form the azeotropic line. Since this equation is approximate and does not take further terms in the expansion into account, the projection of the azeotropic line does not, in general, coincide with the crystallization curve of pure ^4He .

From the crystallization and melting curves of mixtures obtained by us, diagrams of state of ^3He - ^4He mixtures can be plotted for different pressures in the region of low temperatures and small concentrations, where measurements have not been carried out before and there were no data to plot the diagrams in this region. The diagrams plotted are shown in Fig. 6.

As can be seen from the diagrams, a dilute phase exists, not crystallizing at $T = 0$, in the pressure range from the crystallization pressure of pure ^4He , $p = 25$ atm, to the limiting crystallization pressure on the triple line, $p \approx 25.3$ atm. This phenomenon was predicted by Castaing *et al.*⁷ and is connected with the concentration dependence of the limiting

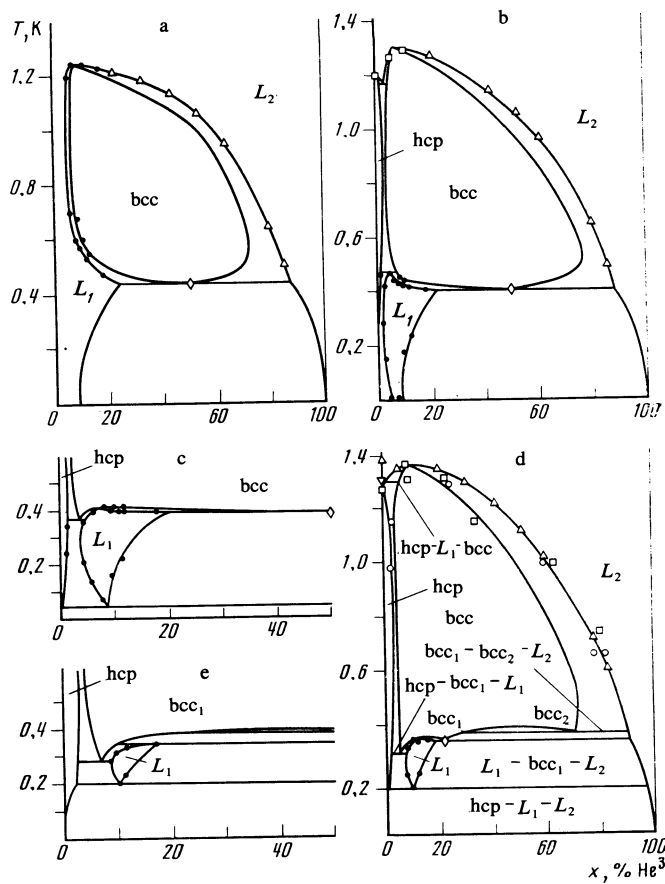


FIG. 6. Phase diagrams of ${}^3\text{He}$ - ${}^4\text{He}$ mixtures for different pressures: a) $p = 24.5$ atm; b) $p = 25.1$ atm; c) $p = 25.3$ atm; d) $p = 25.6$ atm; e) $p = 25.7$ atm. ● results of the present work, Δ) Zinov'eva,¹³ \diamond) Vvedenskii,³ \square) Le Pair *et al.*,¹⁸ \circ) Tedrow and Lee,¹⁶ ∇) Vignos and Fairbank.¹⁷ For designations of the triple lines in Figs a to c, e, see Fig. d.

crystallization pressure of the dilute phase (see Fig. 3).

As the temperature is lowered, on approaching the maximum in the temperature region 0.35–0.4 K, the projections of the crystallization curves on the p - T plane cross (see Fig. 2). At a temperature above the crossing region for constant pressure, the boundary of the region of existence of the dilute phase has a maximum on the high temperature side of the diagrams in the T - x plane, at the peak of which the hcp-bcc- L triple line occurs (Fig. 6b). This triple line will be situated below the maximum at higher pressures, on the side of smaller concentrations (Figs. 6c,d).

At temperatures below the crossing region, liquid with a larger concentration crystallizes at higher pressure; the maximum pressure is then reached on the triple line (Fig. 6e). The maximum on the high temperature side on the T - x diagrams therefore disappears. With decreasing temperature, the curve limiting the dilute phase region, starting from the triple line, first has positive slope which then changes to negative slope at the point $T = 0.28$ K, corresponding to the maximum on the crystallization curves (see Fig. 2).

It follows from the fact that the crystallization curves cross in the p - T plane in the temperature interval 0.35–0.4 K and $p \approx 25.3$ atm, that the crystallization curves at lower

temperatures are situated under the triple line (see Fig. 2). If it is assumed, in agreement with earlier work,^{3,16} that the quadrupole point Q_1 is at the maximum of the bcc- L_1 - L_2 triple line, then it follows from these two statements that the projection of the hcp-bcc- L triple line in the p - T plane at point C crosses the bcc- L_1 - L_2 line and approaches Q_1 from underneath it (see Fig. 4). However, they do not cross in p - T - x space. In T - x diagrams corresponding to higher pressures, the hcp- L_1 -bcc line is lower in temperature than the bcc- L_1 - L_2 line (Fig. 6c-e).

When the bcc phase occurs on triple lines on different sides of the maximum of the curve limiting the dilute L_1 phase (Figs. 6c,d), an azeotropic point will occur at the maximum at which the concentrations of the bcc phase and the dilute liquid phase are the same. According to Vvedenskii's results,³ the ${}^3\text{He}$ concentration in the bcc phase at the L_1 -bcc- L_2 triple line above $T = 0.37$ K is equal to 50% (Figs. 6a-c). The concentration of the bcc phase decreases with increasing pressure (Fig. 6d) and becomes equal to the L_1 concentration at the L_1 -bcc- L_2 triple line at the point where the maximum of the L_1 region disappears. On raising the pressure further, the concentration of the bcc phase becomes less than the concentration of the L_1 phase (Fig. 6e), and at a pressure above the pressure of the quadrupole point Q_1 ($p = 26$ atm), the dilute L_1 phase region disappears.

The study of the crystallization properties of weak ${}^3\text{He}$ - ${}^4\text{He}$ solutions, carried out in the present work, have revealed the existence of maxima on the crystallization curves at $T = 0.28$ K for ${}^3\text{He}$ concentrations up to 17%. At higher concentrations the curves emerge onto the triple line without reaching a maximum. The parabolic form of the curves, $\Delta p \propto T^2$ for $T \rightarrow 0$, determined by the entropy $s_L \propto T$ of only the liquid phase, indicates the practically complete absence of ${}^3\text{He}$ impurity atoms in the crystals. The present measurements of the concentration dependence of the limiting crystallization pressure for $T = 0$, due to the osmotic pressure of the degenerate nonideal Fermi gas of ${}^3\text{He}$ atoms in the solution, agrees well with theoretical results. A ${}^3\text{He}$ - ${}^4\text{He}$ solution with a limiting concentration of about 8% can exist at $T = 0$ without crystallizing up to a pressure of 25.3 atm. Solutions with smaller ${}^3\text{He}$ concentration do not stratify at any temperature. Stratification and reaching the triple line on crystallization at $T = 0$ and at higher temperature occurs for solutions with ${}^3\text{He}$ concentrations above 8%. Melting curves were deduced on the basis of the results obtained and T - x diagrams at constant pressure were plotted.

In conclusion I express my sincere thanks to Yu. D. Anufriev for his help in the discussion of the results, to Academician P. L. Kapitza for enabling the work to be carried out and to V. N. Krutikhin for calibration of the thermometer.

¹E. P. Bashkin and A. E. Meyerovich, *Adv. Phys.* **30**, 1 (1981).

²Yu. D. Anufriev, V. N. Loatik, and A. P. Sebedash, *Pis'ma Zh. Eksp. Teor. Fiz.* **37**, 38 (1983) [*JETP Lett.* **37**, 45 (1983)].

³V. L. Vvedenskii, *Pis'ma Zh. Eksp. Teor. Fiz.* **24**, 152 (1976) [*JETP Lett.* **24**, 132 (1976)].

⁴D. Fenner and K. Luszczynski, *Proc. 14th Int. Conf. Low Temp. Phys. LT-14*, Otaniemi, M. Krusius and M. Vuorio Eds. (1975), Vol. 1, p. 341.

- ⁵G. C. Straty and E. D. Adams, *Phys. Rev.* **150**, 123 (1966).
- ⁶J. Landau, J. T. Tough, N. R. Brubaker, and D. O. Edwards, *Phys. Rev. Lett.* **23**, 283 (1969).
- ⁷B. Castaing, A. S. Greenberg, and M. Papoular, *J. Low Temp. Phys.* **47**, 191 (1982).
- ⁸P. Seligmann, D. O. Edwards, R. E. Sarwinski, and J. T. Tough, *Phys. Rev.* **181**, 415 (1969).
- ⁹J. Landau, J. T. Tough, N. R. Brubaker, and D. O. Edwards, *Phys. Rev. A2*, 2472 (1970).
- ¹⁰J. Bardeen, G. Baym, and D. Pines, *Phys. Rev.* **156**, 207 (1967).
- ¹¹G. Baym and C. Ebner, *Phys. Rev.* **170**, 346 (1968).
- ¹²C. Ebner and D. O. Edwards, *Phys. Rep.* **2C**, 77 (1971).
- ¹³K. N. Zinov'eva, *Zh. Eksp. Teor. Fiz.* **44**, 1837 (1963). [*Sov. Phys. JETP* **17**, 1235 (1963)].
- ¹⁴G. E. Watson, J. D. Reppy, and R. C. Richardson, *Phys. Rev.* **188**, 384 (1969).
- ¹⁵B. van den Brandt, W. Griffioen, G. Frossati, H. van Beelen, and R. de Bruyn Ouboter, *Physica B + C* **114**, 295 (1982).
- ¹⁶P. M. Tedrow and D. M. Lee, *Phys. Rev.* **181**, 1, 399 (1969).
- ¹⁷J. H. Vignos and H. A. Fairbank, *Phys. Rev.* **147**, 185 (1966).
- ¹⁸C. le Pair, K. W. Taconis, R. de Bruyn Ouboter, P. Das, and E. de Jong, *Physica* **31**, 764 (1965).
- ¹⁹V. N. Grigor'ev, B. N. Esel'son, and V. A. Mikheev, *Zh. Eksp. Teor. Fiz.* **66**, 321 (1974) [*Sov. Phys. JETP* **39** 153 (1974)].
- ²⁰L. D. Landau and E. M. Lifshits, *Statistical Physics*, 2nd ed. Pergamon Press, Oxford (1969).
- ²¹M. F. Panczyk, R. A. Scribner, J. R. Gonano, and E. D. Adams, *Phys. Rev. Lett.* **21**, 594 (1968).

Translated by R. Berman